Statistical Model of Railway's Turnout based on Train Induced Vibrations

Barkhordari, Pegah; Galeazzi, Roberto

Published in:
I F A C Workshop Series

Link to article, DOI:
10.1016/j.ifacol.2018.09.570

Publication date:
2018

Document Version
Publisher's PDF, also known as Version of record

Available online at www.sciencedirect.com

ScienceDirect

IFAC PapersOnLine 51-24 (2018) 1278–1284

Statistical Model of Railway's Turnout based on Train Induced Vibrations ⋆

Pegah Barkhordari * **Roberto Galeazzi** **

* *Department of Electrical Engineering, Technical University of Denmark, DK-2800 Kgs. Lyngby, Denmark (e-mail: pebark@elektro.dtu.dk).*
** *Department of Electrical Engineering, Technical University of Denmark, DK-2800 Kgs. Lyngby, Denmark (e-mail: rg@elektro.dtu.dk)*

Abstract: Reliability and dependability of the infrastructure is a must for any railway asset manager to guarantee both safety and capacity of the network. To avoid operational downtime and, even more, accidents timely maintenance of the railway infrastructure becomes a crucial aspect. Current maintenance policies are mostly reactive or periodic, which give surge to a high O&M cost. Reducing maintenance cost while enhancing asset reliability may be achieved through the adoption of predictive maintenance policies. This requires the availability of a condition monitoring system able to assess the infrastructure health state through diagnosis and prognosis of degradation processes occurring on the different railway components. Central to any condition monitoring system is the a-priori knowledge about the process to be supervised in the form of either mathematical models of different complexity or signal features characterizing the health state. This paper proposes a statistical model for the switch panel of railway turnouts that characterizes two key components: railpad and ballast. Exploiting vibration data collected during train passages their natural frequencies are estimated through an estimation scheme based on empirical mode decomposition and subspace identification. By analysing vertical acceleration data corresponding to 400 train passages the estimated resonance frequencies associated with the ballast and the railpad have been well characterized by normally distributed random variables. The proposed estimation architecture and the resulting low-complexity statistical model opens an opportunity for the monitoring of developing degradation processes in the railway's turnout.

Keywords: Statistical modelling, Empirical mode decomposition, Subspace identification, Railway condition monitoring.

1. INTRODUCTION

Continuous availability of the railway network strongly depends on the condition of the infrastructure components. To guarantee network availability and to optimize its performance and capacity condition monitoring and predictive maintenance are of paramount importance. Infrastructure maintenance based on reactive policies has been and still is a major cost driver for railway infrastructure managers that face expenditures for hundreds of millions Euro on a yearly basis to secure safety and availability of the infrastructure (EIM-EFRTC-CER Working Group, 2012; Juul Andersen, 2012).

The maintenance and renewal actions of switches and crossings (S&Cs) contribute significantly to the reported expenses, because S&Cs are critical both in terms of network capacity and safety. Banedanmark, the Danish railway infrastructure manager, estimates that each year one third of the total track maintenance cost is spent on turnouts. According to the 2014 RSSB Annual Safety Performance Report (Clinton, 2014, Section 8.5), 31% of the track-related derailments were caused by S&Cs malfunctioning in the period 2009–2014 in Great Britain. Railway turnouts are complex systems from a geometrical and dynamical point of view, where components of the superstructure (rails and railpads) interact with those of the substructure (ballast and subgrade) to determine the wheel-rail interaction. As such the degradation of one or more of these components directly affects the S&C dynamic performance; in particular failure data recorded in the UK in 2009 (Hassankiadeh, 2011, Chapter 7) showed that ballast degradation is the third most important component with a failing frequency of 7.9 (the first two components affecting turnout performance are the switch rail (45.3%) and the slide chair (30.4%)).

Railway will have a central role in the future development of sustainable transport systems in Europe. This expected key role cannot be guaranteed without optimizing the performance of the infrastructure elements and reducing the maintenance costs associated to faults and failures of turnouts. Therefore, railway infrastructure managers are motivated to change maintenance policies from reactive/periodic to predictive. This can be achieved by devel-

⋆ The financial support under grant number 4109-00003B provided by Innovation Fund Denmark for the INTELLISWITCH project is gratefully acknowledged.

10.1016/j.ifacol.2018.09.570

oping novel condition monitoring (CM) systems capable to issue early warnings of deterioration processes and diagnose occurrence of faults in infrastructure components.

1.1 State of the art

Track stiffness is known as a key parameter to asses the railway condition; in particular noticeable correlation between variations of track stiffness and degradation of railway performance is observed in practice (Berggren et al., 2014). Track stiffness is significantly influenced by the ballast and subgrade condition, therefore their monitoring is crucial to prevent the overall degradation of the infrastructure dynamic behaviour. Evaluation of the "health state" of the ballast by means of non-destructive measurement methods is indeed a challenging task due to the harsh operational conditions. Several approaches were proposed in the literature for condition monitoring of the open track stiffness; these methods can be categorized as *direct* and *indirect*.

Direct methods have been in focus in (Smekal et al., 2006; Berggren, 2009; Kind, 2011; Brough et al., 2003; Labarile et al., 2004; Yella et al., 2009; Asplund et al., 2013) where the ground penetrating radar (GPR), the cone penetration test (CPT) and visual inspection have been considered as means of evaluation of the track condition. Despite being in use across several railway infrastructure managers, these methods have few drawbacks that should be considered in the design of a condition monitoring system: (1) the GPR relies on a proper selection of the frequency range of the electromagnetic waves in order to provide a "good visibility" of the ballast; (2) the CPT is a destructive and time consuming test that influences train operations; (3) the visual inspection is only effective for detection of damage that has already propagated to the surface. Indirect techniques are non-destructive methods that rely on intelligent processing of measured data recorded by track-side or train-based measurement systems. Examples of methods based on measurements collected through train passage are given in (Hosseingholian et al., 2009; Berggren et al., 2014).

Model-based approaches for the detection of degradation of the ballast layer have been recently proposed by Lam et al. (2012, 2014, 2017), who combined complex mechanistic models with Bayesian algorithms for parameter updates. The proposed methods were validated both with simulated and measured acceleration data. The main drawback of these approaches resides on the large dimensionality of the models, which may result in the design of highly complex diagnostic methods. Barkhordari et al. (2017) instead proposed a low-complexity behavioural model of the turnout able to capture the dominant dynamics related to the ballast and the railpad. The fourth-order model was estimated using the Eigenstructure Realization Algorithm (ERA), a subspace identification method, on unloaded vibration data[1] collected during a receptance test. Despite the good prediction capability demonstrated by the identified model when validated against measured vertical track accelerations induced by train passage, the approach proposed in (Barkhordari et al., 2017) relies on the execution of an experimental campaign that railway infrastructure managers very seldom perform.

Low-complexity data-driven behavioural models, which embed the dynamic characteristics of main track components, are industrially appealing since the low parametrization will enable easy tuning and guarantee high portability across the entire railway network despite natural presence of uncertainties due to e.g. geographical location and physical age of the components. Further, the availability of low-complexity models will result in simpler and more robust designs of the monitoring tools for diagnosing faults and prognosing failures.

1.2 Main contribution

This work presents a novel statistical model describing the dynamical features of two key components of the turnout's switch panel: the railpad and the ballast. To overcome the limitations introduced by using data collected through unconventional experimental campaigns in the railway industry – as the receptance test –, the paper proposes a parameter estimation scheme that relies on loaded data, i.e. train induced vertical accelerations, collected by a track side measurement system. The estimation scheme combines the empirical mode decomposition (EMD) with numerical algorithms for subspace state space system identification (N4SID) to estimate second order models for the intrinsic mode functions (IMFs) related to the ballast and the railpad. With the models being available the estimation of the components natural frequencies is achieved through eigenvalue analysis.

The statistical characterization of the parameters describing the dynamical behaviour of the railpad and ballast is deemed necessary in order to take into consideration the presence of uncontrollable external factors – quality of the train's wheels, meteorological conditions, train load and speed – that may determine significant variations in the dynamical response. Exploiting vibration data collected during the passage of 200 IC3 and 200 IR4 trains, the natural frequencies of the ballast and railpad are statistically characterized as normally distributed; further the values estimated based on the receptance test are well within two standard deviations from the mean value.

All measured data presented in the paper are anonymized to comply with the policy of the Danish railway infrastructure manager.

2. EXPERIMENTAL SET-UP

As part of the INTELLISWITCH project a switch and crossing in the Danish railway infrastructure has been instrumented with 3 wheel detectors, 12 2-axis accelerometers (measurement range: ±500g) and 3 displacement sensors (measurement range: ±20mm). All sensors are connected to a cabinet where signals are conditioned and data temporary stored. The location of the sensors along the S&C is shown in the schematics in Fig. 1.

The wheel detectors are used to switch on/off the data collection whenever a train passes through the turnout. The accelerometers are magnetically installed on the rail web

[1] Loaded/unloaded vibration data refer to data collected in the presence/absence of a train loading the infrastructure. Unloaded vibration data are usually collected through a hammer test.

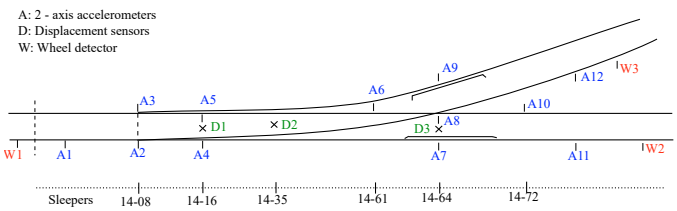

Fig. 1. Layout of the sensors location along the turnout at Tommerup station (Fyn - Denmark). The data utilized in this work refer to vertical accelerations measured by accelerometer A4 on the switch panel.

(a) Overview of the turnout in proximity of Tommerup station

(b) Accelerometer A5 magnetically connected to the rail web

(c) Displacement sensor resting on the sleeper

(d) Wheel detector mounted on proximity of the rail web

Fig. 2. Pictures of the instrumented S&C nearby Tommerup station (Fyn - Denmark).

and measure vertical and lateral accelerations induced by a train passage. The displacement sensors are measuring the vertical motion of the sleepers. The data acquisition board samples all measurements at the sampling frequency $F_s = 20$kHz. Pictures of the instrumented S&C and of selected sensors are shown in Fig. 2.

A turnout is divided in three main areas (along the track): the switch panel, the closure panel and the crossing panel. This work focuses on identifying a low-complexity statistical model of the turnout's dynamics in correspondence of the switch panel. In particular, vertical acceleration measurements at the location of accelerometer A4 (see Fig. 1) are considered for this study. An example dataset is shown in Fig.3, where both the normalized vertical acceleration and the time-shifted output of the wheel detector is reported. The displayed acceleration signal is normalized according to $\bar{a} = a/\max(|a|)$.

The time-shifted output of the wheel detector is utilized to precisely determine when the train boogies are passing through the measurement location A4. The time synchronization between the wheel passage signal $WS(t)$ and the vertical acceleration $\bar{a}(t)$ allows the automatic slicing of the acceleration signal in components referring to

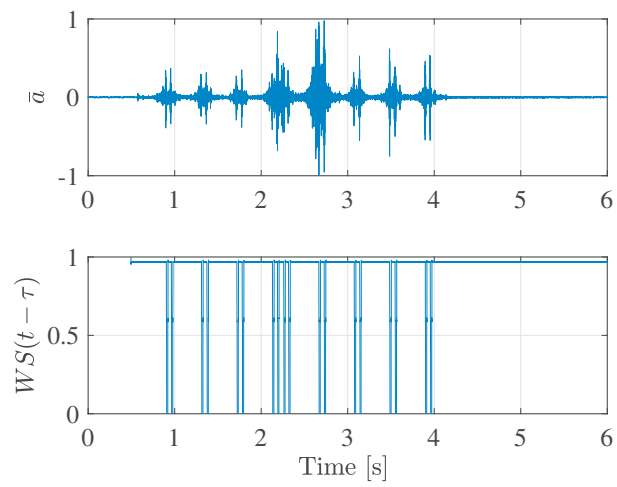

Fig. 3. The track acceleration response to a passenger train (IR4) and the wheel detector signal.

each train boogie for the model identification presented in Section 3. The time delay τ is computed based on the knowledge of the train speed and the distance between the wheel detection sensor and the accelerometer A4.

3. ESTIMATION OF TRACK RESONANCE FREQUENCIES

Condition motoring of the track infrastructure can be performed by continuous evaluation of the track resonance frequencies. Estimation of these resonances from the track response to railway traffic excitation is not a trivial task and advanced signal processing methods should be employed for such a purpose.

The analysis of vertical acceleration time series in correspondence of a boogie (an example shown in Fig. 3) reveals that (1) the signal is not completely damped in between wheels, which implies that the responses to two successive wheels are not fully distinguishable; (2) the maximum amplitude of the acceleration shows significant variation, which may imply issues with the quality of the wheels. Therefore track resonances may be poorly excited and shadowed by other frequencies where the train excitation is more prominent. To lower the impact of spurious measurements on the estimation of the track resonance frequencies, each measured acceleration time series is split into pieces corresponding to the response induced by one boogie. Each piece is then processed independently to give rise to one estimate of the natural frequencies associated with the ballast and the rail pad.

To reliably estimate the track resonance frequencies a novel procedure based on the combination of signal processing and a subspace identification method is proposed. First, empirical mode decomposition is applied to each piece of the acceleration signal to extrapolate the fundamental oscillatory modes included in the signal. Subsequently, the N4SID subspace identification method is used to identify a second order model for each IMF. The models are then exploited to compute the track components natural frequencies by means of eigenvalue analysis. Last the estimated frequencies obtained for all boogies are averaged through the robust statistics of the median. A

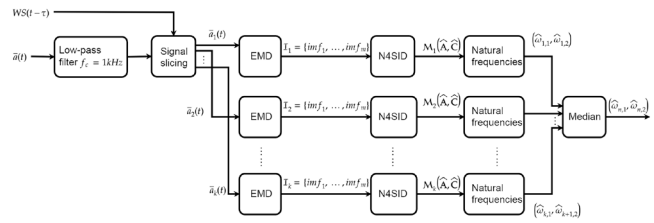

Fig. 4. Block diagram of the estimation scheme for ballast and railpad natural frequencies.

block diagram showing the different stages of the proposed procedure is shown in Fig. 4.

3.1 Empirical Mode Decomposition

Empirical mode decomposition is a signal processing method that decomposes a signal into so-called intrinsic mode functions, which represent the fundamental oscillatory modes of the original signal.

Given a train $\mathcal{T}$ with N_b boogies, let $\mathcal{B} = \{b_1, \ldots, b_{N_b}\}$ be the set of train boogies and $\bar{a}(t)$ for $t \in [t_0, t_1]$ the induced vertical acceleration at a specific location of the turnout. For each b_k the corresponding slice of the overall signal $\bar{a}(t)$ is selected based on the time-shifted output of the wheel sensor, i.e. $\bar{a}_k(t)$ for $t \in [t_{w_1,k}, t_{w_2,k} + \delta]$ is the vertical acceleration induced by the boogie b_k where $t_{w_1,k}$ is the time instant the first wheel passes over the accelerometer, $t_{w_2,k}$ is the time instant the second wheel passes over the sensor and $0 < \delta < t_{w_1,k+1}$. The acceleration $\bar{a}_k(t)$ is the signal fed to the EMD algorithm.

The IMFs are extracted using the sifting process originally presented in (Huang et al., 1998) and summarized in Algorithm 1. The stop conditions in the EMD algorithm (lines 3 and 12) are the following: (1) the overall sifting process stops when the residual $r(t)$ is smaller than a predetermined threshold ϵ_1 or if $r(t)$ has become a monotonic function of time; (2) the sifting process associated with the j-th IMF stops when the standard deviation SD of two consecutive sifting components is smaller than $\epsilon_2 = 0.2 - 0.3$.

The obtained IMFs are then utilized as inputs to the identification process to estimate a low-complexity behavioural model for each train passage.

3.2 N4SID Subspace Identification Method

In (Barkhordari et al., 2017) the identification of a low-complexity behavioural model based on vertical acceleration data collected during a receptance test in unloaded conditions was addressed by exploiting the Eigenstructure Realization Algorithm (ERA). The ERA method assumes that the identification data set represents the dynamics of the system to be identified in free vibration. This hypothesis cannot be met with data collected during train passage for two main reasons: (1) as the train passes over the turnout the infrastructure becomes loaded and this introduces vibrations constraints; (2) the time interval between two successive excitations from two adjacent wheels in a boogie is shorter than the time needed for the measured acceleration to be completely damped. Therefore the

Algorithm 1: Empirical Mode Decomposition

Data: Track vertical acceleration $\bar{a}_k(t)$
Result: Set of intrinsic mode functions $\mathcal{I}_k = \{imf_1, \ldots, imf_m\}$

1 Residual $r(t) \leftarrow \bar{a}_k(t)$;
2 $i \leftarrow 1$;
3 **while** $r(t) > \epsilon_1$ **do**
4 $\quad h_{10}(t) \leftarrow r(t)$;
5 $\quad j \leftarrow 1$;
6 $\quad$ **repeat**
7 $\quad\quad$ Find all local extrema $h_{1(j-1)}(t)$;
8 $\quad\quad$ Find the upper and lower envelopes by spline interpolation of the local extrema;
9 $\quad\quad$ Compute the mean value $m(t)$ between the lower and upper envelopes;
10 $\quad\quad$ Subtract the mean value from the original signal $h_{1j}(t) = h_{1(j-1)}(t) - m(t)$;
11 $\quad\quad$ Compute

$$SD = \sum_{t=t_{w1,k}}^{t_{w2,k}+\delta} \frac{|h_{1(j-1)}(t) - h_{1j}(t)|^2}{h_{1j}^2(t)}$$

$\quad\quad$ $j \leftarrow j + 1$;
12 $\quad$ **until** $SD > \epsilon_2$;
13 $\quad imf_i(t) \leftarrow h_{1(j-1)}(t)$;
14 $\quad r(t) \leftarrow r(t) - imf_i(t)$;
15 $\quad i \leftarrow i + 1$;
16 **end**

N4SID algorithm for state space system identification is employed.

This subspace identification method was proposed for LTI systems in order to identify a state space model representing the input/output behaviour of a system (Viberg, 1995). For the j-th IMF extracted from the EMD algorithm, the past and future output data in the N4SID algorithm (i.e. $\mathbf{Y}_p$ and $\mathbf{Y}_f$) are constructed as $\mathbf{Y}_p = (imf_j)_{0|k-1}$ and $\mathbf{Y}_f = (imf_j)_{k|2k-1}$. Since the input signal (train excitation) is unknown, the past and future input vectors in the identification procedure (i.e. $\mathbf{U}_f$ and $\mathbf{U}_p$) are set to zero. Defining $\mathbf{W}_p$ as $[\mathbf{U}_p \ \mathbf{Y}_p]^T$, the N4SID identification algorithm read (Katayama (2006))

(1) Compute the oblique projection of $\mathbf{Y}_f$ onto $\mathbf{W}_p$ along $\mathbf{U}_f$ (i.e. ξ) by using Eq. (1) and the LQ decomposition in Eq. (2)

$$\xi = \hat{\mathbf{E}}_{||\mathbf{U}_f}\{\mathbf{Y}_f|\mathbf{W}_p\} = \mathbf{R}_{32}\mathbf{R}_{22}^{\dagger}\mathbf{W}_p = \mathbf{O}_k\mathbf{X}_f \quad (1)$$

$$\begin{bmatrix} \mathbf{U}_f \\ \mathbf{W}_p \\ \mathbf{Y}_f \end{bmatrix} = \begin{bmatrix} \mathbf{R}_{11} & \mathbf{0} & \mathbf{0} \\ \mathbf{R}_{21} & \mathbf{R}_{22} & \mathbf{0} \\ \mathbf{R}_{31} & \mathbf{R}_{32} & \mathbf{0} \end{bmatrix} \begin{bmatrix} \bar{\mathbf{Q}}_1^T \\ \bar{\mathbf{Q}}_2^T \\ \bar{\mathbf{Q}}_3^T \end{bmatrix}, \quad (2)$$

where $\mathbf{R}_{22}^{\dagger}$ is the pseudo-inverse of $\mathbf{R}_{22}$. $\mathbf{O}_k$ is the extended observability matrix and $\mathbf{X}_f$ is the future state vector.

(2) Compute the state vector $\mathbf{X}_f$ using the singular value decomposition of ξ (see Eq. (4)) and define $\bar{X}_{k+1}, \bar{X}_k, \bar{Y}_{k|k}, \bar{U}_{k|k}$.

$$\xi = \mathbf{U}_1\mathbf{\Sigma}_1\mathbf{V}_1^T = \mathbf{O}_k\mathbf{X}_f \tag{3}$$
$$\mathbf{O}_k = \mathbf{U}_1\mathbf{\Sigma}_1^{\frac{1}{2}}\mathbf{T}$$
$$\mathbf{X}_f = \mathbf{T}^{-1}\mathbf{\Sigma}^{\frac{1}{2}}{}_1\mathbf{V}_1^{-1},$$

where $\mathbf{X}_f = [x(k), x(k+1), ..., x(k+N-1)] \in \mathbb{R}^{n\times N}$.

(3) Compute the matrices $\hat{\mathbf{A}}, \hat{\mathbf{B}}, \hat{\mathbf{C}}, \hat{\mathbf{D}}$ by solving the regression equation using least-squares techniques.

$$\begin{bmatrix}\hat{\mathbf{A}} & \hat{\mathbf{B}}\\ \hat{\mathbf{C}} & \hat{\mathbf{D}}\end{bmatrix} = \left(\begin{bmatrix}\bar{\mathbf{X}}_{k+1}\\ \mathbf{Y}_{k|k}\end{bmatrix}\begin{bmatrix}\bar{\mathbf{X}}_k\\ \bar{\mathbf{U}}_{k|k}\end{bmatrix}^T\right)\left(\begin{bmatrix}\bar{\mathbf{X}}_k\\ \bar{\mathbf{U}}_{k|k}\end{bmatrix}\begin{bmatrix}\bar{\mathbf{X}}_k\\ \bar{\mathbf{U}}_{k|k}\end{bmatrix}^T\right)^{-1} \tag{4}$$

where $\bar{\mathbf{X}}_{k+1} \in \mathbb{R}^{n\times N-1}$ is the estimated future states, $\mathbf{Y}_{k|k} \in \mathbb{R}^{p\times N-1}$ is the future output data, $\bar{\mathbf{U}}_{k|k} \in \mathbb{R}^{m\times N-1}$ is the future input data.

3.3 Frequency Estimation

For the j-th IMF a canonical realization of the second order discrete-time state space model can be defined as follows,

$$\begin{cases}\hat{\mathbf{x}}_j(k+1) = \hat{\mathbf{A}}_j\hat{\mathbf{x}}_j(k)\\ \hat{\mathbf{y}}_j(k) = \hat{\mathbf{C}}_j\hat{\mathbf{x}}_j(k)\end{cases}. \tag{5}$$

$\hat{\mathbf{A}}_j$ and $\hat{\mathbf{C}}_j$ are defined in terms of natural frequency (ω_n) and damping factor (ζ) in the following equation,

$$\hat{\mathbf{A}}_j = exp(\begin{bmatrix}0 & 1\\ -\omega_n^2 & -2\zeta\omega_n\end{bmatrix} \times T_s)\ ,\ \hat{\mathbf{C}}_j = [1\ 0]\,. \tag{6}$$

The resonance frequency and the damping factor corresponding to the model identified for the j-th IMF can be computed by means of eigenvalue analysis

$$w_{nj} = \frac{|\ln(\lambda_1(\hat{\mathbf{A}}_j))|}{2\pi T_s},\quad \zeta_j = \frac{-\mathrm{Re}(\ln(\lambda_1(\hat{\mathbf{A}}_j))/T_s)}{|\ln(\lambda_k(\hat{\mathbf{A}}_j))|}, \tag{7}$$

where T_s is the sampling time and $\lambda_1(\hat{\mathbf{A}}_j)$ is the first eigenvalue of the complex pair associated with the matrix $\hat{\mathbf{A}}_j$.

4. LOW-COMPLEXITY BEHAVIOURAL MODEL

By applying the methodology proposed in the previous section to the measured track vertical acceleration in response to train passages, a low-complexity behavioural model capturing the ballast and railpad dynamics of the turnout is now developed. According to the literature (see e.g. (Dahlberg, 2006)) and the analysis of the receptance test presented in (Barkhordari et al., 2017), the frequency interval containing the resonance frequencies of the track infrastructure is $[0, 1000]$Hz. Therefore, the measured data is pre-filtered using a low-pass filter with the cut-off frequency of 1000 Hz. As discussed in Section 3, the filtered acceleration response is then split into time segments corresponding to a boogie. For each time segment the EMD algorithm is used to produce IMFs, which in turn are considered as an identification data set. The N4SID method is then applied to each identification dataset for identifying a proper state space model representing the dominant behaviour of the measured acceleration. According to the literature (Dahlberg, 2006) the first and second resonance frequencies of the track corresponding to the flexibility of the ballast and railpad are found in the ranges of $[50\,,\,300]$ Hz and $[200\,,\,600]$ Hz, respectively.

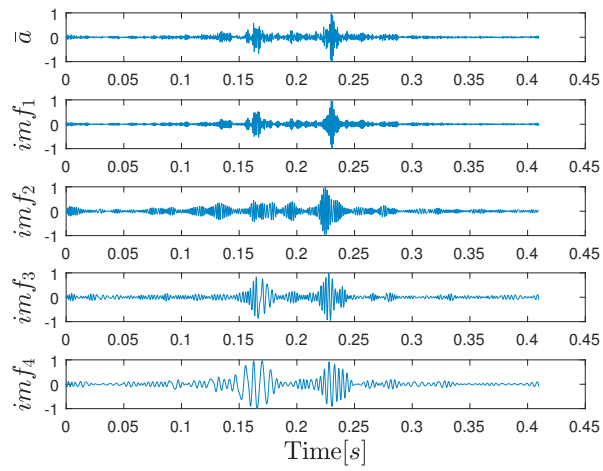

Fig. 5. Track response to a passage of two adjacent wheels (IR4 train travelling at 158km/h) and the four extracted IMFs.

Since each IMF represents one simple oscillatory mode of the original signal, a 2nd order model is identified for each IMF.

Figure 5 shows an example of the acceleration response recorded for a passage of two adjacent wheels and the four IMFs extracted. Performing the latter analysis for each IMF, it can be shown that only the excited frequencies calculated for the second and fourth IMFs are within the frequency range in which the track resonance frequencies are expected.

4.1 Model Validation and Robustness

The discrete time state space realization of the identified models for imf_2 and imf_4 associated with the data set shown in Fig. 5 are

$$\mathcal{M}_2 : \begin{cases}\hat{\mathbf{A}}_2 = \begin{bmatrix}0.9976 \pm 0.1845e^{-3} & 0.0592 \pm 0.1787e^{-3}\\ -0.0592 \pm 0.1787e^{-3} & 0.9976 \pm 0.1845e^{-3}\end{bmatrix}\\ \hat{\mathbf{C}}_2 = \begin{bmatrix}0.7073 \pm 0.6536e^{-4} & -0.0209 \pm 0.6352e^{-4}\end{bmatrix}\end{cases} \tag{8}$$

$$\mathcal{M}_4 : \begin{cases}\hat{\mathbf{A}}_4 = \begin{bmatrix}0.9812 \pm 0.4030e^{-3} & 0.1757 \pm 0.3918e^{-3}\\ -0.1757 \pm 0.3918e^{-3} & 0.9812 \pm 0.4030e^{-3}\end{bmatrix}\\ \hat{\mathbf{C}}_4 = \begin{bmatrix}0.7082 \pm 0.1449e^{-3} & -0.0627 \pm 0.1405e^{-3}\end{bmatrix}\end{cases} \tag{9}$$

$\mathcal{M}_2$ and $\mathcal{M}_4$ are then combined through the output into a unified model $\mathcal{M}$ able to predict the dominant behaviour of the measured acceleration in relation to the ballast and railpad components

$$\mathcal{M} : \begin{cases}\hat{\mathbf{A}} = \begin{bmatrix}\hat{\mathbf{A}}_2 & \mathbf{0}\\ \mathbf{0} & \hat{\mathbf{A}}_4\end{bmatrix}\\ \hat{\mathbf{C}} = \begin{bmatrix}\hat{\mathbf{C}}_2 & \hat{\mathbf{C}}_4\end{bmatrix}\end{cases}. \tag{10}$$

It is worth noting that since the train load (input to the model) is not available for measurement, the output is estimated by using only the $\hat{\mathbf{A}}$ and $\hat{\mathbf{C}}$ matrices. Therefore, the initial conditions are required to be estimated iteratively for each wheel passage.

To assess the robustness of the final model, its capability in predicting the measured accelerations in response to

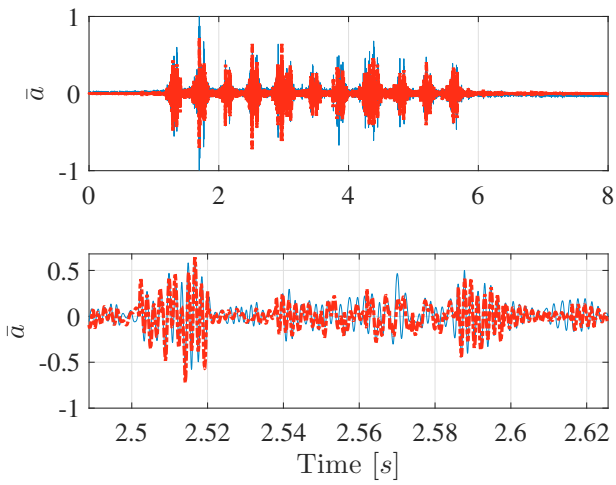

Fig. 6. Comparison of the measured (blue) and predicted accelerations (red) in correspondence to an IR4 train passage at 120km/h. (Top) The whole train passage, (Bottom) Zoomed in of a boogie passage.

another train excitation recorded at the turnout position A4 is evaluated. The comparison between measured acceleration and predicted output is shown in Fig. 6 and the fitting score is 77% for this particular dataset.

5. STATISTICAL CHARACTERISTIC OF THE TRACK RESONANCES

To find a single value representing the first (second) resonance frequency of the track subject to train passage, the median calculated over all observations (i.e., all values extracted as first (second) frequency from different time segments) is taken into account. In other words, median of all extracted $\omega_{n,i1}$ and $\omega_{n,i2}$, where i is the time segments counter, is calculated. The first and second resonances obtained based on the analysis of the track response shown in Fig. 5 are only one sample among many others. Therefore, acceleration response of the track to a pool of train excitations (200 IC3 trains and 200 IR4 trains with the speed ranging from 120 km/h to 160km/h) has been used for further analysis. The described estimation procedure is then applied to the recorded track acceleration responses and a probability density function (PDF) is found for each resonance frequency.

Figures 7-10 show the PDF and the probability plot for the first and second resonances. The vertical dashed-line in these figures represents the track resonance computed by using the receptance test data Barkhordari et al. (2017). Using the Kolmogorov-Smirnov (K-S) goodness-of-fit test with a confidence level of 95%, the p-value is calculated as, 0.719, 0.2248, 0.4213 and 0.0522 for the fitted normal distributions. This emphasizes that statistical characteristic of the track resonances can be represented as normal distribution. The mean value of the PDFs in these figures are close to the first and second resonances of the track obtained in Barkhordari et al. (2017), by performing a receptance test at the Tommerup station ($\omega_{n,1} = 167.59$Hz and $\omega_{n,2} = 549.96$ Hz).

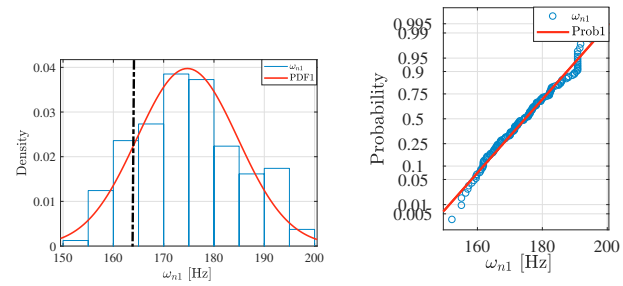

(a) probability density function (b) probability plot

Fig. 7. Statistical characteristic of the first track resonance; IC3 trains.

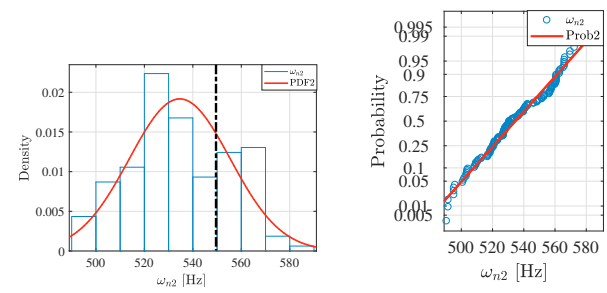

(a) probability density function (b) probability plot

Fig. 8. Statistical characteristic of the second track resonance; IC3 trains.

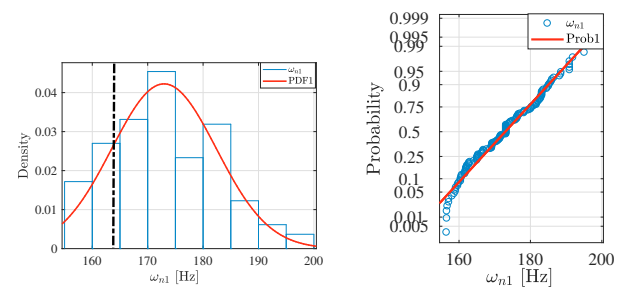

(a) probability density function (b) probability plot

Fig. 9. Statistical characteristic of the first track resonance; IR4 trains.

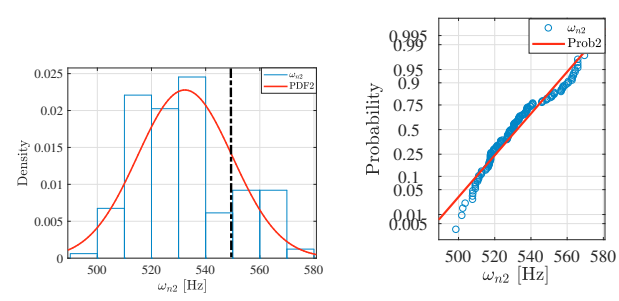

(a) probability density function (b) probability plot

Fig. 10. Statistical characteristic of the second track resonance; IR4 trains.

5.1 Discussion

The method proposed in this paper can be employed successfully to generate the statistical description of railway track resonances using vibration data relative to train passage. The statistical model provides a robust description of the infrastructure dominant behaviour in relation to uncontrollable parameters as train speed, wheel load, environmental conditions, etc. Further, the statistical model may be exploited for long-term monitoring of infrastructure characteristics through e.g. recursive updating of the obtained PDFs. Last, the statistical model opens for wide opportunities to design novel change detectors to address the occurrence of faults and/or wear at the ballast and railpad level. These methods will be inherently data-driven to increase the portability of the condition monitoring system across different S&Cs in the railway network.

6. CONCLUSION

A low-complexity behavioural model capable of predicting the dynamic response of a railway turnout around the switch panel was identified by using the measured track vertical acceleration. This was carried out by proposing a novel estimation scheme based on the combination of the empirical mode decomposition and the N4SID subspace identification method. The model identified for the track response to a train passage was then employed to estimate railway track resonances. The robustness and validity of the model were demonstrated by testing the capability of the identified model to predict the dominant behaviour of a new set of data measured during the passage of a different train. Statistical properties of the resonance frequencies were then obtained by considering a pool of IR4 and IC3 trains, and finding a probability density function fitted to each resonance frequency. The findings of the current study can be used as a basis for portable and predictive condition monitoring of railway switches and crossings.

REFERENCES

Asplund, M., Larsson, D., Rantatalo, M., Nissen, A., and Kumar, U. (2013). Inspection of railway turnouts using camera. In *Proceedings of the 10th World Congress on Railway Research*. Australia.

Barkhordari, P., Galeazzi, R., de Miguel Tejada, A., and Santos, I. (2017). Low-complexity behavioral model for predictive maintenance of railway turnouts. In *2017 Annual Conference of the Prognostics and Health Management Society*.

Berggren, E. (2009). *Railway Track Stiffness - Dynamic Measurements and Evaluation for Efficient Maintenance*. Phd thesis, Royal Institute of Technology.

Berggren, E., Nissen, A., and Paulsson, B. (2014). Track deflection and stiffness measurements from a track recording car. *Proceedings of the Institution of Mechanical Engineers, Part F: Journal of Rail and Rapid Transit*, 228(6), 570–580.

Brough, M., Stirling, A., Ghataora, G., and Madelin, K. (2003). Evaluation of railway trackbed and formation: a case study. *NDT & E International*, 36(3), 145–156.

Clinton, A. (2014). Annual Safety Performance Report 2013/14. Technical report, Railway Safety and Standards Board.

Dahlberg, T. (2006). handbook of railway vehicle dynamics . *von S. Iwnicki. Taylor & Francis Group*, 143–179.

EIM-EFRTC-CER Working Group (2012). Market strategies for track maintenance & renewal. Technical Report 2353 7473-11, CER - Community of European Railway and Infrastructure Companies.

Hassankiadeh, S. (2011). *Failure Analysis of Railway Switches and Crossings for the purpose of Preventive Maintenance*. Msc thesis, Royal Institute of Technology.

Hosseingholian, M., Froumentin, M., and Levacher, D. (2009). Continuous method to measure track stiffness a new tool for inspection of rail infrastructure. *World Applied Sciences Journal*, 6(5), 579–589.

Huang, N.E., Shen, Z., Long, S.R., Wu, M.C., Shih, H.H., Zheng, Q., Yen, N.C., Tung, C.C., and Liu, H.H. (1998). The empirical mode decomposition and the hilbert spectrum for nonlinear and non-stationary time series analysis. In *Proceedings of the Royal Society of London A: mathematical, physical and engineering sciences*, volume 454, 903–995. The Royal Society.

Juul Andersen, K. (2012). Årsrapport 2012. Technical Report 13-00144, banedanmark.

Katayama, T. (2006). *Subspace methods for system identification*. Springer Science & Business Media.

Kind, T. (2011). GPR antenna array for the inspection of railway ballast. In *Proceedings of the National Seminar & Exhibition on Non-Destructive Evaluation*.

Labarile, A., Stella, E., Ancona, N., and Distante, A. (2004). Ballast 3D reconstruction by a matching pursuit based stereo matcher. In *Proceedings of the 2004 IEEE Intelligent Vehicles Symposium*, 653–657. IEEE.

Lam, H., Alabi, S., and Yang, J. (2017). Identification of rail-sleeper-ballast system through time-domain Markov chain Monte Carlo-based Bayesian approach. *Engineering Structures*, 140, 421–436.

Lam, H., Hu, Q., and Wong, M. (2014). The Bayesian methodology for the detection of railway ballast damage under a concrete sleeper. *Engineering Structures*, 81, 289–301.

Lam, H., Wong, M., and Yang, Y. (2012). A feasibility study on railway ballast damage detection utilizing measured vibration of in situ concrete sleeper. *Engineering Structures*, 45, 284–298.

Smekal, A., Berggren, E., and Silvast, M. (2006). Monitoring and substructure condition assessment of existing railway lines for upgrading to higher axle loads and speeds. In *Proceedings of the 7th World Congress on Railway Research*. Canada.

Viberg, M. (1995). Subspace-based methods for the identification of linear time-invariant systems. *Automatica*, 31(12), 1835–1851.

Yella, S., Dougherty, M., and Gupta, N. (2009). Condition monitoring of wooden railway sleepers. *Transportation Research Part C: Emerging Technologies*, 17(1), 38–55.